Hierarchy of Supramolecular Arrangements and Building Blocks: Inverted Paradigm of Crystal Engineering in the Unprecedented Metal Coordination of Methylene Blue

Inorganic Chemistry

Article

pubs.acs.org/IC

# Hierarchy of Supramolecular Arrangements and Building Blocks: Inverted Paradigm of Crystal Engineering in the Unprecedented Metal Coordination of Methylene Blue

Stefano Canossa,[†] Alessia Bacchi,[†] Claudia Graiff,[†,‡] Paolo Pelagatti,[†,‡] Giovanni Predieri,*[,†,‡] Andrea Ienco,[§] Gabriele Manca,[§] and Carlo Mealli*[,§]

[†]Dipartimento di Chimica, Università degli Studi di Parma, Area delle scienze 17/A, 43124 Parma, Italy

[§]ICCOM-CNR, Via Madonna del Piano 10, 50019 Sesto Fiorentino, Florence, Italy

[‡]Consorzio Interuniversitario Reattività Chimica e Catalisi, Via Celsio Ulpiani 27, 70126 Bari, Italy

Supporting Information

**ABSTRACT:** The aromatic methylene blue cation ($MB^+$) shows unprecedented ligand behavior in the X-ray structures of the trigonal-planar (TP) complexes $MBMCl_2$ (M = $Cu^I$, $Ag^I$). The two isostructural compounds were exclusively synthesized by grinding together methylene blue chloride and MCl solids. Only in the case of AuCl did the technique lead to a different, yet isoformular, $Au^I$ derivative with separated $MB^+$ and $AuCl_2^-$ counterions and no direct N−Au linkage. While the density functional theory (DFT) molecular modeling failed in reproducing the isolated Cu and Ag complexes, the solid-state program *CRYSTAL* satisfactorily provided for Cu the correct TP building block associated with a highly compact $\pi$ stacking of the $MB^+$ ligands. In this respect, the dispersion interactions, evaluated with the DFT functional, provide to the system an extra energy, which likely supports the unprecedented metal coordination of the $MB^+$ cation. The feature seems governed by subtle chemical factors, such as, for instance, the selected metal ion of the coinage triad. Thus, the electronically consistent $Au^I$ ion does not form the analogous TP building block because of a looser supramolecular arrangement. In conclusion, while a given crystalline design is generally fixed by the nature of the building block, a peculiarly efficient supramolecular packing may stabilize an otherwise unattainable metal complex.

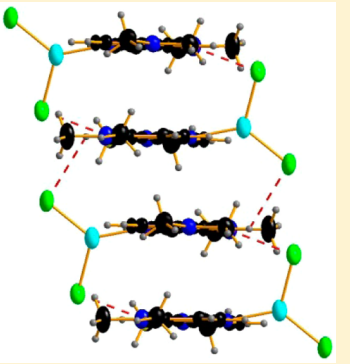

## INTRODUCTION

Methylene blue (MB) is a salt of the formula $[(C_{16}H_{18}SN_3)^+Cl^-]$ [IUPAC name: 3,7-bis(dimethylamino)-phenothiazin-5-ium chloride]. The $MB^+$ cation consists of three condensed six-membered rings and two coplanar $NMe_2$ substituents. The aromaticity is suggested by the total 18 $p_\pi$ electron count, as indicated from the resonant structures in Scheme 1.

A qualitative molecular orbital (MO) picture[1] corroborates the donor weakness of the phenothiazine N atom, given that its in-plane $\sigma$ lone pair lies well below the frontier MO region. The lowest unoccupied MO is instead an accessible $\pi^*$ level, favoring the N-atom reduction to an amide, with the system's puckering due to the lost aromaticity. The acquired N basicity[2,3] is also consistent with the known N−H/N−R derivatives,[4] also stable in the monoxidized form.[5,6] For the redox reversibility, promoted by the alternative glucose and $O_2$ reactants and the associated color change, MB is often used as an indicator.[7] Other applications are in photocatalysis[8,9] and enzyme-catalyzed redox reactions. As a drug, MB is employed for treating diseases such as methemoglobinemia,[10] cyanide,[11,12] carbon monoxide poisoning,[13] malaria,[14−16] and Alzheimer's.[17] In these fields, the combination of MB with a metal center could be, in principle, advantageous, but its coordination capabilities remain elusive in the literature. Perhaps, the closest example of bonding to a metal is in the crystal structure of $MB^+[HgCl_3]^-$,[18] although the N−Hg distance of 2.779 Å exceeds the sum of the covalent radii as well as the average value, evaluated from the Cambridge database.[19] Other invoked cases of $MB^+$ coordination to a metal are even more speculative in the lack of structural characterization.[20,21]

This paper provides the first evidence of the $MB^+$ ligand behavior based on the structures of the three-coordinated complexes $[(MBMCl_2]$ with M = $Cu^I$ or $Ag^I$. Support from

**Scheme 1. Resonant Structures of the 18e$^-$ Aromatic $MB^+$ [a]**

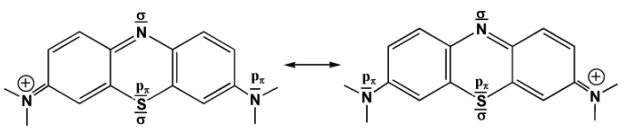

[a]Electron pairs at the heteroatoms are distinguished for their $p_\pi$ or $\sigma$ character.

**Received:** December 20, 2016




DOI: 10.1021/acs.inorgchem.6b02980
*Inorg. Chem.* XXXX, XXX, XXX−XXX

suitable density functional theory (DFT) calculations is also provided when taking into account crystalline supramolecular interactions. Among the latter, the London dispersion forces play a decisive role in some sterically encumbered organic compounds, as emphasized by a recent review article.[22] The role is instead much less considered for transition-metal complexes, concerning, in particular, possible effects on metal coordination. A conclusion reached by this study is that the supramolecular interactions, among which is the $\pi$ stacking of aromatic units, can end up conferring unknown coordination capabilities to an unsuited species such as $MB^+$.

## RESULTS AND DISCUSSION

Only by using a mechanochemical strategy was the synthesis of complexes $[(MBCuCl_2]$ and $[(MBAguCl_2]$ (simplified as MBCu and MBAg) successfully achieved. This implied the grinding together of the solid methylene blue chloride pentahydrate and CuCl or AgCl. Conversely, the equivalent combination of reactants in solution failed. The progress of the reactions was monitored by powder X-ray diffraction (PXRD) analysis. In the case of Cu, the traces of the starting reagents disappeared completely after 30 min of grinding without the addition of a solvent's drop. In the case of Ag, a few drops of acetone had to be added to complete the reaction within 20 min. In both cases, the color changed from dark green to reddish brown, while some PXRD traces of the final powders indicated the attainment of new crystalline phases (Figure 1).

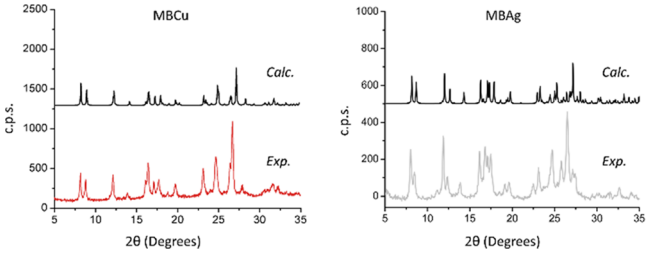


**Figure 1.** Experimental and calculated PXRD patterns of MBCu and MBAg products. Distinct positions of the experimental and calculated signals likely depend on the temperature of the data collection (298 and 100 K for PXRD and single-crystal diffraction, respectively).

Suitable crystals for X-ray analyses were isolated upon slow evaporation of the dimethylformamide (MBCu) and acetonitrile (MBAg) solutions of the ground solids. As shown in Figure 1, the recorded PXRD patterns coincide with those calculated from the determined single-crystal X-ray structures.[23] Select geometric parameters of the isostructural MBCu and MBAg compounds are shown in Table 1, where the values in brackets are those of the MBCu optimization with *CRYSTAL*.[24]

Approximate trigonal-planar (TP) metal complexes are formed by the two $Cl^-$ and the $MB^+$ ligands. This result is surprising because, in general, a cationic ligand hardly forms an uncharged metal complex.[25−28] The behavior of $MB^+$ as a $2e^-$ donor is corroborated by the relatively short N−M linkages of 1.987(4) and 2.329(5) Å in the Cu and Ag compounds, respectively. The Ag coordination is comparatively less effective because the N−Ag bond is larger than the sum of the covalent radii and the average value from all of the corresponding CCDC structures.[19] The point is also supported by the somewhat more open Cl−Ag−Cl angle (119.48° vs 113.73°). In no case is the $Cl_2M$ fragment either coplanar or orthogonal to the $MB^+$ plane, thus excluding any higher symmetry of the

**Table 1. Experimental Geometric Parameters (Å and deg) of the Isostructural Complexes $(MB)MCl_2$ (M = Cu, Ag)[a]**

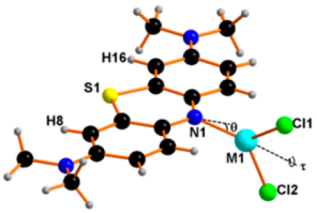


| | MBCu | MBAg |
|---|---|---|
| M1−Cl1 | 2.2220(5) [2.18] | 2.4425(19) |
| M1−Cl2 | 2.2494(5) [2.19] | 2.4659(18) |
| M1−N1 | 1.9874(13) [1.91] | 2.329(5) |
| Cl1−M1−Cl2 | 113.739(18) [111.0] | 119.48(6) |
| Cl1−M1−N1 | 129.45(4) [126.8] | 125.09(13) |
| Cl2−M1−N1 | 116.70(4) [122.2] | 115.32(13) |
| $\theta$ | 11.8(4) [2.5] | 9.5(2) |
| $\tau$ | 75.2(2) [57.6] | 66.8(2) |

[a]The values in square brackets are for the Cu model, optimized with *CRYSTAL*.[24]

complexes. The corresponding $\tau$ rotation of $Cl_2M$ about the N−M linkage has intermediate values of 75.2 and 66.8° for MBCu and MBAg, respectively. Another important parameter, defined in Table 1, concerns the out-of-plane shift of the metal from the $MB^+$ plane, which is almost equivalent in the two complexes (angles 11.8° and 9.5°). However, $\tau$ rotation has consequences on the extended heap, formed by the parallel $MB^+$ units in an alternating head-to-tail arrangement (Figure 2).

First of all, the view down the N−M vector (Figure 2a) highlights the "leaning tower" shape of the heap, consistent with the continuous lateral sliding of each complex unit by a half condensed hexagon. In this manner, the atoms of two adjacent $MB^+$ cations do not eclipse each other. Conversely, Figure 2b clarifies the role of the $\tau$ and $\theta$ angles for the whole system. The $Cl_2M$ rotation shortens the contact between any Cl atom and one H−C group of one adjacent $MB^+$ cation. This allows single but continuous hydrogen-bonding interactions with an apparent stabilization of the heap. On the other hand, the latter cannot be pairwise equivalent because of the $\theta$ deviation, which favors one Cl···H−C interaction with respect to the subsequent one. In fact, the Cl···H distances are as different as 2.614 and 2.89 Å and 2.622 and 2.816 Å in MBCu and MBAg, respectively. As a major consequence, the heap's building block cannot be a single complex but one of two alternative dimers. The first one features two N−M vectors, which simultaneously point toward the associated $MB^+$ unit (green box in Figure 2b), while the vectors diverge in the dimer formed by the two central complexes (red box). The two possible building blocks have different interplanar distances of 3.506 vs 3.403 Å and 3.485 vs 3.307 Å in MBCu and MBAg, respectively. Remarkably, the dimer with the closer contacts between the cations is the one with larger Cl···H−C contacts. This suggests an inverse correlation between the main supramolecular forces ($\pi$−$\pi$ and hydrogen bonding), as further discussed in the computational part.

The compound MBAu, formed by the third coinage metal (gold), was similarly synthesized by grinding together ~~with~~ the solid reactants MB and Au(tht)Cl (tht = tetrahydrothiophene). Five cycles of solvent-assisted grinding were necessary to


DOI: 10.1021/acs.inorgchem.6b02980
Inorg. Chem. XXXX, XXX, XXX−XXX

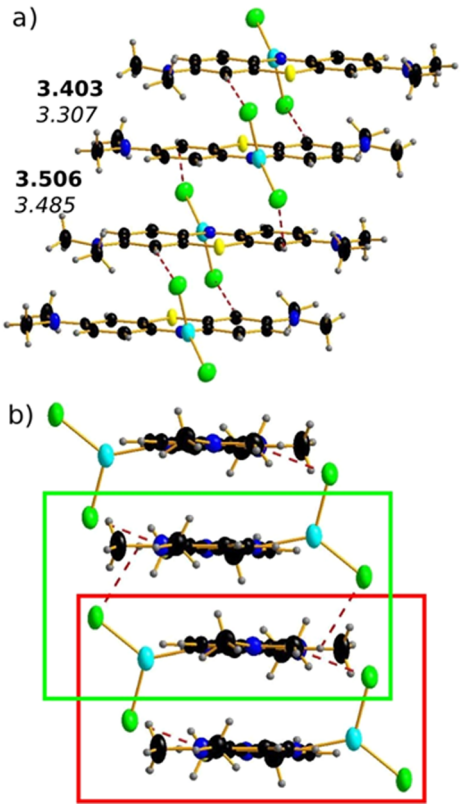


**Figure 2.** Layered MBCu and MBAg complexes. (a) View down the N−M linkages, highlighting the "leaning tower" shape of the heap. (b) Orthogonal view down the largest $MB^+$ dimension, showing the two possible dimeric building blocks in the boxes.

completely convert the starting materials into a new crystalline phase, as evidenced by the PXRD monitoring of the reaction (see the Supporting Information, PXRD3−5). In this manner, the concomitant formation of a crystalline gold metal phase also emerged, as shown by new signals in place of those attributed to the target phase. Crystals suitable for X-ray analysis were obtained upon the slow evaporation of a filtered dichloromethane solution of the powder.

f3 The X-ray structure of MBAu in Figure 3 is indicative of a salt of formula $[(MB^+)(AuCl_2^-)]$. In fact, the N−Au separation of 4.201 Å excludes $MB^+$ coordination because it is corroborated by the quasi-linearity of the $AuCl_2^-$ anion (angle of 177.57°). Discrete ion pairs may also be excluded because the metal fragments form hydrogen bonds with distinct

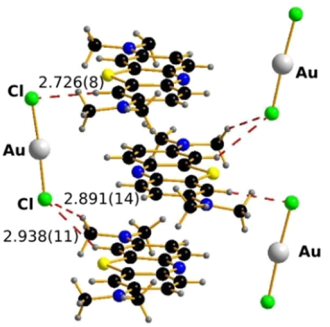


**Figure 3.** Packing features of the MBAu crystalline phase,[23] showing Cl···H contacts between linear $AuCl_2^-$ fragments and $MB^+$ molecules.

counterions and $\pi$ stacking holds the parallel $MB^+$ units together in a head-to-tail arrangement.

The now larger interplanar separation of 3.599 Å is indicative of weaker interactions between the planes, also because the adjacent cations are now shifted by one entire six-membered ring. The reduced lattice energy is therefore likely insufficient to compensate for the difficult formation of the N−$Au^I$ coordination bond.[29] Examples of the latter are rare and not well-defined, with one example being a T-shaped species with a P−Au−S linear moiety associated with an orthogonal pyridine ligand, which remains 2.56 Å far from the metal.[30] On the other hand, the propensity of the $d^{10}$ coinage metals to add a third coplanar ligand diminishes down the triad, as found for a $P_2MCl$ series ($P_2$ = chelate diphosphine) with the progressively larger Cl separation.[31]

Some authors attributed the different behavior of Au to relativistic effects,[32] which remained elusive when included in some of our DFT calculations. The latter were initially based on the molecular modeling of the single $MBMCl_2$ complexes (M = Cu, Ag) carried out with the B3LYP-DFT[33] method both in the gas phase and in a $CHCl_3$ solvent.[34,35] Unfortunately, these optimizations were not consistent with the X-ray structural data. Only Cu apparently formed a three-coordinated complex with the $MB^+$ ligand, but its geometry was clearly incorrect. Not only were the N−Cu distance and the Cl−Cu−Cl angle overestimated by about +0.15 Å and +32°, respectively, but the metal was far from lying on the $MB^+$ plane ($\theta$ = 49°). MBAg optimization was even less performing because a N···Ag separation of >6.0 Å excluded the existence of the coordination bond, consistently with a quasi-linear $Cl_2Ag^-$ fragment (170°). In this respect, MBAg seemed more similar to MBAu than the MBCu compound, which was similarly optimized. At this point, it became evident that the neglected intermolecular forces could have a role in the $MB^+$ coordination, as was already implicit in the spectroscopic analysis of the MBCu and MBAg compounds in an acetonitrile solution. In fact, no NMR or MS signal was attributable to the possible N−Cu or N−Ag coordination.

Evidence for supramolecular forces at work in the extended heap of $MBCuCl_2$ units emerged from the solid-state calculations with the program *CRYSTAL*.[24] Before going into the details, it is worth mentioning that the stacking had been explored at the molecular level for the single dimeric building block of Figure 2b. Remarkably, the standard B3LYP[33] calculations indicated immediate scission of the single complexes, which attain the mentioned incorrect geometry. Conversely, the dispersion correction in the B97D functional[36] afforded an acceptable optimization of the $(MBCuCl_2)_2$ assembly with two in-pointing N−Cu vectors, although with a $\theta$ angle of 23.8° (Figure S4), which shortens the Cl···H−C interactions (ave. 2.48 Å). Interestingly, a third stacked complex (Figure 4) restores the experimental $\theta$ value of 11° at the f4 central unit but not at the terminal ones (16° and 29°). This problem of boundary conditions disappears in the solid-state approach.

The *CRYSTAL* optimization with the B97D functional shows an acceptable geometry of the stacked complex units (see the values in brackets in Table 1). Also, the "leaning tower" aspect of the heap is well reproduced (Figure S5a) with distinct and alternating dimeric building blocks, although with smaller and similar interplanar separations (3.10 and 3.06 Å). To evaluate the effect, likely attributable to the dispersion forces, a new *CRYSTAL* optimization was attempted at the BLYP level. At


DOI: 10.1021/acs.inorgchem.6b02980
Inorg. Chem. XXXX, XXX, XXX−XXX

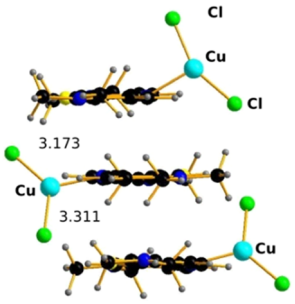


**Figure 4.** DFT-optimized assembly of three $MBCuCl_2$ complexes.

first sight, the structure (Figure S5b) was better behaving, especially for the larger and more asymmetric interplanar separations of 3.41 and 3.30 Å. However, this result is associated with a questionable stereochemistry, given that the rotation of each $Cl_2Cu$ fragment about the N−Cu linkage is in the opposite sense (negative $\tau$ angle). Consequently, the Cl−S contacts are preferentially shortened with respect to the Cl···H−C ones. This suggests a residually positive S atom in $MB^+$, possibly consistent with resonance structures rather than those in Scheme 1. In any case, the stereochemical conflict between the optimized and experimental structures kept us from further exploring the problem.

The combined strategy of molecular and solid-state modeling offered the possibility of deriving useful energy data on the interaction between adjacent complexes.[37] On average, the enthalpy of the attraction is about −40 kcal $mol^{-1}$, mostly because of the dispersion forces. In fact, the dismissal of the latter in the BLYP approach transforms the interaction into a minor repulsion (∼+2 kcal $mol^{-1}$). Therefore, $\pi$ stacking has a governing role and overwhelms other contributions such as hydrogen-bonding or residual electrostatic attraction between differently charged counterions at different complexes. Consider in this respect that the components of the latter type are equally included in the two adopted functionals, without any major evidence of their specific contribution in favoring the assembly of the planar and formally closed-shell complexes.

To support the still scarcely documented role of the packing forces in assisting metal coordination, we mention a previous study reported by some of us (C.M. and A.I.)[38,39] on $Mn^{II}$ dimers with four carboxylate bridges and a terminal bipyridine (bipy) chelate per metal. In these species, the local metal coordination was trigonal-prismatic, while in the crystal, the unsubstitued bipy ligands were involved in extended and compact $\pi$ stacking. However, the introduction of some methyl substituent at bipy induces a major structural effect, such as the forcing of an octahedral $Mn^{II}$, also because the $CH_3$ substituents do not allow the same effective $\pi$ stacking of the planar chelates. In fact, the loss of lattice energy (although unvalued by calculations) cannot support the trigonal-prismatic coordination anymore. With respect to the latter case, the present $MB^+$ behavior seems even more remarkable because $\pi$ stacking controls not only the coordination geometry but also Werner's coordination number[40] (from 2 to 3).

## CONCLUSION

In conclusion, the coordination capabilities of the aromatic $MB^+$ cation have been assessed for the first time. Analyses have shown that the supramolecular forces govern the overall stereochemistry to the point of affording in some cases otherwise disfavored and still unknown complexes of MB. Because the latter compound already has a relevant number of applications in different areas of chemistry, it cannot be excluded that some new fruitful usage may be derived in combination with a transition-metal center. For this reason, the synthetic procedures, stereochemistry, and electronic underpinnings of our solid-state systems may represent a useful guideline in the search for new supramolecular systems, where MB (or a similar synthon) is associated with various metal centers. In this respect, an added value of this paper is the mechanochemical technique used, in place of other standard synthetic strategies in solution. Hopefully, the formation of other highly energetic supramolecular patterns may offer important perspectives for chemistry.

## ASSOCIATED CONTENT

### Supporting Information

The Supporting Information is available free of charge on the ACS Publications website at DOI: 10.1021/acs.inorgchem.6b02980.

X-ray crystallographic data in CIF format (CIF)
Experimental details on the syntheses of the compounds at issue, IR and PXRD characterization data, the CCDC search outcome on the N−Cu and N−Ag coordination length bonds, and drawings and coordinates of computed structures (PDF)

## AUTHOR INFORMATION

### Corresponding Authors

*E-mail: giovanni.predieri@unipr.it.
*E-mail: carlo.mealli@iccom.cnr.it.

### ORCID

Alessia Bacchi: 0000-0001-5675-9372
Paolo Pelagatti: 0000-0002-6926-2928
Giovanni Predieri: 0000-0002-7912-641X

### Author Contributions

This paper received contributions of all the authors. These authors contributed with the DFT calculations and the further interpretation of the computed results.

### Notes

The authors declare no competing financial interest.

## ACKNOWLEDGMENTS

The CNR of Trieste, and in particular Dr. Nicola Demitri, is gratefully acknowledged for the single-crystal X-ray diffraction data collected at the ELETTRA synchrotron facility. The CREA Center and Project HP10CHEVJ8 (CINECA) are thanked for computational resources.

## DEDICATION

Dedicated to Antonio Tiripicchio on the occasion of his 80th birthday.

## REFERENCES

(1) Mealli, C.; Proserpio, D. M. MO Theory made visible. *J. Chem. Educ.* **1990**, *67*, 399.
(2) Filip, I. H.; Gál, E.; Lupan, I.; Perde-Schrepler, M.; Lönnecke, P.; Surducan, M.; Găină, L. I.; Hey-Hawkins, E.; Silaghi-Dumitrescu, L. Tuning the coordination properties of phenothiazine by regioselective introduction of diphenylphosphanyl groups. *Dalton Trans.* **2015**, *44*, 615−629.


DOI: 10.1021/acs.inorgchem.6b02980
*Inorg. Chem.* XXXX, XXX, XXX−XXX

(3) Kumar, V.; Upadhyay, N.; Manhas, A. Designing, syntheses, characterization, computational study and biological activities of silver-phenothiazine metal complex. *J. Mol. Struct.* **2015**, *1099*, 135−141.
(4) Edema, J. J. H.; Gambarotta, S.; Meetsma, A.; Spek, A. L.; Smeets, W. J. J.; Chiang, M. Y. Chromium (II) amides: synthesis and structures. *J. Chem. Soc., Dalton Trans.* **1993**, 789−797.
(5) Rosokha, S. V.; Kochi, J. K. Continuum of outer-and inner-sphere mechanisms for organic electron transfer. Steric modulation of the precursor complex in paramagnetic (ion-radical) self-exchanges. *J. Am. Chem. Soc.* **2007**, *129*, 3683−3697.
(6) Okamoto, T.; Kuratsu, M.; Kozaki, M.; Hirotsu, K.; Ichimura, A.; Matsushita, T.; Okada, K. Remarkable Structure Deformation in Phenothiazine Trimer Radical Cation. *Org. Lett.* **2004**, *6*, 3493−3496.
(7) Cook, A. G.; Tolliver, R. M.; Williams, J. E. The Blue Bottle Experiment Revisited: How Blue? How Sweet? *J. Chem. Educ.* **1994**, *71*, 160.
(8) Kim, W.; Jang, G.; Lee, J.; Rhee, D. Degradation of Methylene Blue by Titania Doped with Transition Metal and Nitrogen. *Energy Procedia* **2014**, *61*, 2456−2459.
(9) Bergamonti, L.; Alfieri, I.; Lorenzi, A.; Montenero, A.; Predieri, G.; Di Maggio, R.; Girardi, F.; Lazzarini, L.; Lottici, P. P. Characterization and photocatalytic activity of TiO2 by sol−gel in acid and basic environments. *J. Sol-Gel Sci. Technol.* **2015**, *73*, 91−102.
(10) Cawein, M.; Behlen, C. H.; Lappat, E. J.; Cohn, J. E. Hereditary Diaphorase Deficiency and Methemoglobinemia. *Arch. Intern. Med.* **1964**, *113*, 578−585.
(11) Wendel, W. B. Methylene blue, methemoglobin, and cyanide poisoning. *Pharmacol. Exp. Ther.* **1935**, *54*, 283−298.
(12) Hanzlik, P. J. Methylene Blue as Antidote for Cyanide Poisoning. *JAMA* **1933**, *100*, 357.
(13) Brooks, M. M. Methylene blue as an antidote for cyanide and carbon monoxide poisoning. *JAMA* **1933**, *100*, 59.
(14) Guttmann, P.; Ehrlich, P. Berl. Ueber die Wirkung des Methylenblau bei Malaria. Berliner klinische. *Klin. Wochenschr.* **1891**, *28*, 953−956.
(15) Coulibaly, B.; Zoungrana, A.; Mockenhaupt, F. P.; Schirmer, R. H.; Klose, C.; Mansmann, U.; Meissner, P. E.; Muller, O. Strong gametocytocidal effect of methylene blue-based combination therapy against falciparum malaria: a randomised controlled trial. *PLoS One* **2009**, *4*, e5318.
(16) Färber, P. M.; Arscott, L. D.; Williams, C. H., Jr; Becker, K.; Schirmer, R. H. Recombinant Plasmodium falciparum glutathione reductase is inhibited by the antimalarial dye methylene blue. *FEBS Lett.* **1998**, *422*, 311−314.
(17) Wischik, C. M.; Edwards, P. C.; Lai, R. Y.; Roth, M.; Harrington, C. R. Selective inhibition of Alzheimer disease-like tau aggregation by phenothiazines. *Proc. Natl. Acad. Sci. U. S. A.* **1996**, *93*, 11213−11218.
(18) Raj, M. M.; Dharmaraja, A.; Kavitha, S. J.; Panchanatheswaran, K.; Lynch, D. E. Mercury(II)-methylene blue interactions: Complexation and metallate formation. *Inorg. Chim. Acta* **2007**, *360*, 1799−1808.
(19) *Cambridge Structural Database System*, version 5.32; Cambridge Crystallographic Data Centre, Cambridge, U.K.
(20) Jonnalagadda, S. B.; Gollapalli, N. R. Speciation and stability of methylene blue-metal-thiocyanate ion-association complexes. *Bull. Chem. Soc. Ethiop.* **2008**, *22*, 85−91.
(21) Moawed, E. A.; Zaid, M. A. A.; El-Shahat, M. F. Methylene Blue-Grafted Polyurethane Foam Using as a Chelating Resin for Preconcentration and Separation of Cadmium(II), Mercury(II), and Silver(I) from Waste Water. *Anal. Lett.* **2003**, *36*, 405−421.
(22) Wagner, J. P.; Schreiner, P. R. London Dispersion in Molecular Chemistry—Reconsidering Steric Effects. *Angew. Chem., Int. Ed.* **2015**, *54*, 12274−12296.
(23) CCDC 1475865 (MBCu), 1475866 (MBAg), and 1481894 (MBAu) contain the supplementary crystallographic data for this paper. These data are provided free of charge by The Cambridge Crystallographic Data Centre.
(24) Dovesi, R.; Orlando, R.; Erba, A.; Zicovich-Wilson, C. M.; Civalleri, B.; Casassa, S.; Maschio, L.; Ferrabone, M.; De La Pierre, M.; D'Arco, P.; Noel, Y.; Causa, M.; Rerat, M.; Kirtman, B. CRYSTAL14: A Program for the Ab initio Investigation of Crystalline Solids. *Int. J. Quantum Chem.* **2014**, *114*, 1287−1317.
(25) Goedken, V. I.; Vallarino, L. M.; Quagliano, J. V. Cationic Ligands. Coordination of the 1,1,1-Trimethylhydrazinium Cation to Nickel(II). *Inorg. Chem.* **1971**, *10*, 2682−2685.
(26) Mercer, D. D. J. W.; Jenkins, H. A. Cationic ligands for Ag(I): Organometallic polymers versus unimolecular complexes. *Inorg. Chim. Acta* **2007**, *360*, 3091−3098.
(27) Emmert, M. H.; Brannon, G. J.; Villalobos, J. M.; Sanford, M. S. Platinum and palladium complexes containing cationic ligands as catalysts for arene H/D exchange and oxidation. *Angew. Chem., Int. Ed.* **2010**, *49*, 5884−5886.
(28) Sailaja, S.; Swarnabala, G.; Rajasekharan, M. V. Complexes of $Ag^{I}$ with cationic ligands: bis[(pyridylmethyl)ammonio]silver(I) salts. *Acta Crystallogr., Sect. C: Cryst. Struct. Commun.* **2001**, *57*, 1162−1165.
(29) Abdou, H. E.; Mohamed, A. A.; Fackler, J. P., Jr. Synthesis and X-ray structures of dinuclear and trinuclear gold (I) and dinuclear gold (II) amidinate complexes. *Inorg. Chem.* **2005**, *44*, 166−168.
(30) Kuz'mina, L. G.; Grandberg, K. I.; Il'ina, L. G. Synthesis and crystal structure of [(2-methoxyphenylimino)(2-pyridyl)-methylthiolato](triphenylphosphine)gold(I). *Russ. J. Inorg. Chem.* **1995**, *40*, 182.
(31) Barrow, M.; Bűrgi, H. B.; Johnson, D. K.; Venanzi, M. L. Coordination geometries and bond types in three-coordinate phosphine complexes of copper(I), silver(I), and gold(I). *J. Am. Chem. Soc.* **1976**, *98*, 2356−2357.
(32) Pyykkö, P. Relativistic effects in structural chemistry. *Chem. Rev.* **1988**, *88*, 563−594.
(33) (a) Becke, A. D. Densityfunctional thermochemistry. III. The role of exact exchange. *J. Chem. Phys.* **1993**, *98*, 5648−5652. (b) Lee, C.; Yang, W.; Parr, R. G. Development of the Colle-Salvetti correlation-energy formula into a functional of the electron density. *Phys. Rev. B: Condens. Matter Mater. Phys.* **1988**, *37*, 785−789.
(34) (a) Barone, V.; Cossi, M. Quantum Calculation of Molecular Energies and Energy Gradients in Solution by a Conductor Solvent Model. *J. Phys. Chem. A* **1998**, *102*, 1995−2001. (b) Cossi, M.; Rega, N.; Scalmani, G.; Barone, V. Energies, structures, and electronic properties of molecules in solution with the C-PCM solvation model. *J. Comput. Chem.* **2003**, *24*, 669−681.
(35) The B3LYP and B97D functionals employed were tested; the Stuttgart−Dresden and LANL2DZ pseudopotentials were used for metal atoms. For $Au^{I}$, the Douglas−Kroll−Hess second-order scalar relativistic approach did not afford significant changes of the geometric and stereochemical parameters.
(36) Grimme, S. Semiempirical GGA-type density functional constructed with a long-range dispersion correction. *J. Comput. Chem.* **2006**, *27*, 1787−1799.
(37) Single-point calculations were carried out with *Gaussian* at both the B97D and B3LYP levels on molecular models consisting of one, two, and four stacked complexes with their structures optimized by *CRYSTAL*. This allowed estimations of the interaction energies in each dimer and between pairs of dimers.
(38) Grirrane, A.; Pastor, A.; Galindo, A.; Ienco, A.; Mealli, C.; Rosa, P. First example of a tetra-carboxylate bridged dimanganese species. *Chem. Commun.* **2003**, 512−513.
(39) (a) Grirrane, A.; Pastor, A.; Galindo, A.; del Rio, D.; Orlandini, A.; Mealli, C.; Ienco, A.; Caneschi, A.; Fernandez Sanz, J. Supramolecular Interactions as Determining Factors of the Geometry of Metallic Building Blocks: Tetracarboxylate Dimanganese Species. *Angew. Chem., Int. Ed.* **2005**, *44*, 3429−3432. (b) Grirrane, A.; Pastor, A.; Galindo, A.; Alvarez, E.; Mealli, C.; Ienco, A.; Orlandini, A.; Rosa, P.; Caneschi, A.; Barra, A.-L.; Fernandez Sanz, J. Thiodiacetate−Manganese Chemistry with N ligands: Unique Control of the Supramolecular Arrangement over the Metal Coordination Mode. *J. Chem. - Eur. J.* **2011**, *17*, 10600−10617.
(40) Bowman-James, K. Alfred Werner revisited: the coordination chemistry of anions. *Acc. Chem. Res.* **2005**, *38*, 671−678.


DOI: 10.1021/acs.inorgchem.6b02980
*Inorg. Chem.* XXXX, XXX, XXX−XXX